Research Article

Nano Research
2022, 15(4): 3614–3620

ISSN 1998-0124 CN 11-5974/O4
https://doi.org/10.1007/s12274-021-3906-x

Direct stamping multifunctional tactile sensor for pressure and temperature sensing

Binghao Liang[1,§], Bingfang Huang[1,§], Junkai He[1], Rongliang Yang[1], Chengchun Zhao[1], Bo-Ru Yang[1] (✉), Anyuan Cao[2], Zikang Tang[3], and Xuchun Gui[1] (✉)

[1] *State Key Laboratory of Optoelectronic Materials and Technologies, School of Electronics and Information Technology, Sun Yat-sen University, Guangzhou 510275, China*
[2] *Department of Materials Science and Engineering, College of Engineering, Peking University, Beijing 100871, China*
[3] *Institute of Applied Physics and Materials Engineering, University of Macau, Avenida da Universidade, Taipa, Macau, China*
[§] *Binghao Liang and Bingfang Huang contributed equally to this work.*

© Tsinghua University Press and Springer-Verlag GmbH Germany, part of Springer Nature 2021

Received: 24 July 2021 / **Revised:** 22 September 2021 / **Accepted:** 26 September 2021

ABSTRACT

Flexible and wearable sensors have broad application prospects in health monitoring and artificial intelligence. Many different single-functional sensing devices have been developed in recent years, such as pressure sensors and temperature sensors. However, it is still a great challenge to design and fabricate tactile sensors with multiple sensing functions. Herein, we propose a simple direct stamping method for the fabrication of multifunctional tactile sensors. It can detect pressure and temperature stimuli signals simultaneously. This pressure/temperature sensor possesses high sensitivity (0.67 kPa^{-1}), large linear range (0.75–5 kPa), and fast response speed (15.6 ms) in pressure sensing. It also has a high temperature sensitivity (1.41%/°C) and great linearity (0.99) for temperature sensing in the range of −30 to 30 °C. All these excellent performances indicate that this pressure/temperature sensor has great potential in applications for artificial intelligence and health monitoring.

KEYWORDS

pressure sensing, temperature sensing, carbon nanotube, direct stamping

1 Introduction

In recent years, flexible and wearable tactile sensors [1–5] have attracted tremendous interest due to their great potential in health monitoring and human-machine interaction. Many different kinds of single functional sensors such as pressure sensors [6–15], strain sensors [16–20], temperature sensors [21], and humidity sensors [22] have been reported recently. Based on the fast development of single functional sensors, more and more attention has shifted to the fabrication of multifunctional sensors which can measure more than one kind of stimuli [23]. Since pressure sensing and temperature sensing are two of the most important functions of human skin, multifunctional sensors which can detect pressure and temperature signals simultaneously have been widely studied and have much significant progress.

Pressure/temperature sensors can be divided into two classes: One is that a single sensor has both pressure and temperature sensing functions [24–27] and the other is a single device assembled by pressure sensing and temperature sensing elements [28, 29]. For the first type, for instance, porous carbon and polydimethylsiloxane (PDMS) composite-based sensors can realize pressure sensing and temperature sensing in a single sensor [30]. More multifunctional sensors are the second type, which was designed and fabricated by vertically stacking pressure sensors and temperature sensors [31, 32]. In both multifunctional sensors, when measuring both pressure stimuli and temperature stimuli in one sensor, the coupling and distinguishing of two signals is critical and challenging. It is hard to measure and identify two input signals by a single output. Therefore, to avoid the interference of stimuli, multifunctional sensing devices were usually fabricated by integrating different sensors in one device. However, the integration process of two or more sensors is complicated and the multifunctional sensing devices fabricated by this stacking strategy were usually too thick for electronic skin application. Although great efforts have been made in multifunctional sensors, the coupling of different stimuli and the complicated integration technologies are still impeding the development of multifunctional sensors.

Generally, the performance of the sensor depends on the structure and sensitive layer, which transforms the stimuli into an electrical signal. Recently, many methods have been developed for the fabrication of conductive sensitive layers. For example, after dispersing conductive nanomaterials in organic solutions, a conductive sensitive layer film can be easily fabricated on polymer substrates by dip-coating [33, 34], spin-coating [35–37], direct printing technology [38–41], etc. However, the dispersion process of conductive materials will cause damage to their structure and change in properties. Therefore, it is necessary to develop some dry fabrication processes for the fabrication of conductive sensitive layers for multifunctional tactile sensors.

Stamp, similar to typography technology, has been widely used in official documents for thousands of years. During the stamping process, the seal adsorbs and transfers liquid ink onto the target

Address correspondence to Bo-Ru Yang, yangboru@mail.sysu.edu.cn; Xuchun Gui, guixch@mail.sysu.edu.cn

substrate. Afterward, the pattern will be printed on the substrate. Herein, inspired by the stamp, a versatile dry transfer method was developed to fabricate pressure/temperature sensors, which can sense pressure stimuli and temperature stimuli through different electrodes in a signal device. By directly stamping carbon nanotube (CNT) and spin coating poly(3,4-ethylenedioxythiophene):poly(4-styrenesulfonate) (PEDOT:PSS) onto Ecoflex substrate, we can fabricate a conductive sensitive layer with high efficiency and low cost for the tactile sensors. The sensor possesses high sensitivity (0.67 kPa^{-1}) for pressure sensing. It also shows a high temperature coefficient of resistance (TCR), which is suitable for high sensitivity temperature sensors (1.41%/°C). Besides, the sensor possesses great stability (5,000 cycles) and a fast response speed (15.6 ms) in pressure sensing. Potential applications in rapid mouse click monitoring, pressure mapping, and tiny pressure detection are demonstrated, which indicates the application prospect of our pressure/temperature sensor.

2 Experimental section

2.1 Fabrication of CNT film

The CNT sponge was synthesized by chemical vapor deposition as reported in our previous work [42]. The micro-structured Ecoflex substrate was fabricated by mixing the A and B components (with volume ratio 1:1) of silicone rubber gel (Smooth-On, Ecoflex 00-30). The liquid state Ecoflex was poured and coated on the surface of silicon carbide sandpaper. After curing at room temperature for 24 h, the micro-structured Ecoflex substrate, with a thickness of 300 μm, can be separated from the sandpaper. The CNT film was transferred to the substrate by a home-made stamping system.

2.2 Fabrication of pressure/temperature sensor

PEDOT:PSS was transferred to the CNT film by spin coating to form a PEDOT:PSS/CNT conductive layer. The anodic aluminum oxide (AAO) membranes with a thickness of 1.0 μm were obtained from Top-membranes Technology Co., Ltd. CNT film, AAO membranes, and PEDOT:PSS/CNT thin film was then stacked and assembled to fabricate a sandwich structure pressure/temperature sensor.

2.3 Device characterization

Scanning electron microscopy (SEM) images of CNT film and pressure/temperature sensor were characterized using a Hitachi S-4800 field emission scanning electron microscope. Optical microscopy images were captured using a Carl Zeiss Axio CSM 700 confocal light microscope. The electrical properties of the pressure/temperature sensor were measured by a Keithley 2400 digital multi-meter at a test voltage of 0.1 V. The performance of the pressure/temperature sensor was characterized by a home-made system consisting of a force gauge (Mark 1-, M5-025) and a programmable linear stage (Zolix, TSA100). The temperature response performance was mainly characterized at room temperature (20 °C).

3 Results and discussion

The fabricating process of the CNT conductive film is illustrated in Fig. 1(a). A porous CNT sponge was mounted on a force meter, which can move in the vertical direction. The Ecoflex substrate was attached to the conveyor which can move in the horizontal direction. First, the target area of the Ecoflex substrate was transferred by the conveyor to the printing area under the CNT sponge. After that, the CNT sponge (served as both seal and ink) was pressed on the substrate under a pressure of 100 kPa. Since the adhesion interaction between the Ecoflex substrate and the CNT sponge was stronger than the interaction between the nanotubes, after separation, a layer of CNT film was left on the surface of the Ecoflex substrate. Due to its abundant polar groups, the Ecoflex substrate exhibits strong adhesive characteristics to CNTs, which enable various interactions at the interface of substrate and CNTs, including van der Waals, and electrostatic interactions [43]. The prepared CNT film is very uniform throughout the stamp range, similar to the stamp by a stone seal with the words of "SYSU" (inset of Fig. 1(a)). The morphology and sheet resistance of the CNT films fabricated by the same parameters are relatively consistent, as reported in our previous work [43]. By adjusting the stamping pressure, we can control the performance and thickness of the transferred CNT film. With the increase of stamp pressure, the thickness of the CNT film will be increased, resulting in a decrease in sheet resistance and transmittance [43]. This CNT film preparing method is simple, high-efficiency, eco-friendly and energy-saving, which makes it suitable for continuous fabrication in mass. For example, the continuous fabricating system (Fig. 1(b)), which consists of two programmable linear motors for moving substrate and CNT seal, and a force meter for controlling the pressure, can prepare several CNT films in just one minute.

Because CNT sponge has a porous structure and a very low

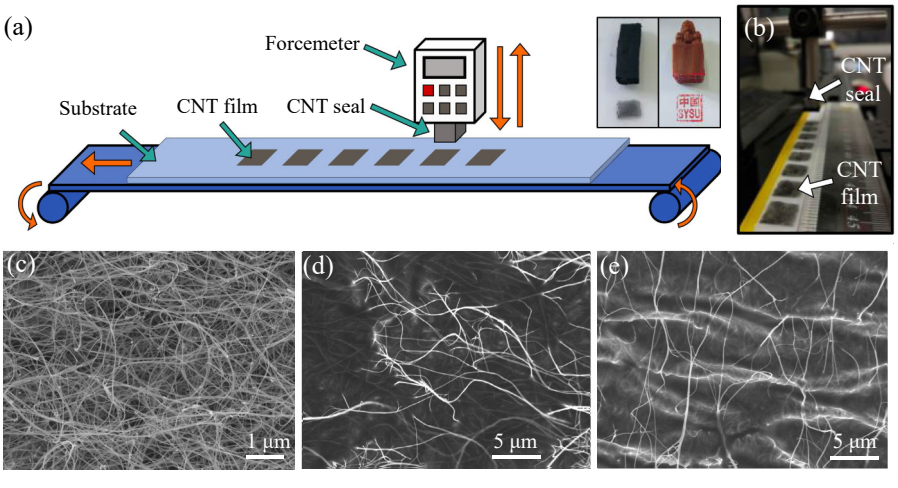

Figure 1 Schematic illustration of the fabricating process and characterization of as-prepared CNT films. (a) Schematic illustration of the stamping system (inset: photographs of the CNT seal and stone seal). (b) Photograph of the home-made continuous stamping system and as-prepared CNT films. (c) SEM image of CNT sponge seal. (d) SEM image of the fabricated CNT film on smooth Ecoflex substrate. (e) SEM image of the fabricated CNT film on rough Ecoflex substrate.

density, the van der Waals' interaction between the individual carbon nanotube is weak, which makes it easier to transfer the CNT from the bulk material to the substrate. The microstructure of the CNT sponge was characterized by SEM, as shown in Fig. 1(c). It shows that the CNT in the sponge self-assembled into a porous and interconnected framework. The length of the CNT reaches several hundred microns. This characteristic ensures that the transferred CNT film has a homogeneous network structure. As shown in the SEM image (Fig. 1(d)), after being transferred onto a flat Ecoflex substrate, the CNT network is continuous and uniform. The thickness of the CNT film is about tens of nanometers. Since it is on a flexible Ecoflex substrate, it is difficult to accurately determine its thickness. By this direct dry transfer technology, we can also transfer CNT film to a target substrate with a rough surface or micro-structured surface. For example, we have fabricated a surface micro-structured Ecoflex substrate by using commercialized sandpaper as a template. After the direct dry stamping process, a uniform CNT network can be transferred to this substrate (Fig. 1(e)).

With this continuous CNT film direct fabrication technology, we have designed and fabricated a multifunctional sensor, which can measure pressure and temperature simultaneously. The fabricating process of this multifunctional sensor is illustrated in Fig. S1 in the Electronic Supplementary Material (ESM). First, by using a piece of sandpaper as a template, an Ecoflex substrate with Gaussian distribution surface microstructure was fabricated. Then, a layer of CNT film was transferred to the Ecoflex substrate by the dry stamping method. The CNT/Ecoflex film was served as one of the electrodes in the pressure/temperature sensor. By spin coating PEDOT:PSS on another CNT/Ecoflex film, a PEDOT:PSS/CNT/Ecoflex composite film was fabricated and served as the other electrode for the sensor. Since the PEDOT:PSS/CNT film possesses a much larger temperature coefficient, it could serve as a temperature sensing material as well. Then, a layer of AAO membrane was then transferred between two electrodes for isolating the electrodes by polymethyl methacrylate (PMMA)-assisted method [44]. Finally, silver wires were connected on both ends of the CNT electrode and PEDOT:PSS/CNT electrode to form a sandwich structure pressure/temperature sensor.

The structure of the pressure/temperature sensor is schematically illustrated in Fig. 2(a). The AAO membrane with microholes is served as a blocking layer. The CNT electrode and PEDOT:PSS/CNT electrodes are separated by the blocking layer to avoid initial current in order to save energy and improve the sensitivity. The equivalent circuit is shown in Fig. 2(b). By monitoring the resistance of the PEDOT:PSS/CNT layer between electrode In_1 and Out_1, we can measure the temperature signal. On the other hand, the resistance R_c between In_1 and Out_2 depends on the applied pressure. The working mechanism of the pressure sensor is illustrated in Fig. 2(c). Two layers of electrodes are separated by the AAO membrane before pressing the sensor. When the pressure is applied, the electrodes will be compressed and deformed. Connections between two layers of the electrode will form and current will flow through the microholes of the AAO membrane. With the increasing applied pressure, the contact area between two electrodes will be enlarged and the current will increase simultaneously. The surface microstructure of Ecoflex substrate before and after the CNT film transferred is demonstrated in Fig. 2(d) and Fig. S2 in the ESM. As shown in the SEM images, the height profile of the Ecoflex substrate follows the Gaussian distribution which can largely extend the linear range of the pressure sensor. Some recent papers also confirmed that the linearity of the pressure sensor can be improved by introducing the surface microstructure [2]. The SEM images (Figs. S2(c) and S2(d) in the ESM) show that CNT can completely follow the surface microstructure of the Ecoflex substrate. The AAO membrane can completely cover the CNT film and be supported by the cone of the microstructured substrate, as shown in the right half of Fig. 2(e). The diameter of the micro-holes in the AAO membrane is about 300 nm, as shown in Fig. 2(f), and Figs. S2(e) and S2(f) in the ESM.

Figure 3(a) shows the current response of the pressure/temperature sensor under an applied pressure up to 12 kPa. As the pressure increases, the response current increases nearly linearly. As shown in the inset of Fig. 3(a), under the applied pressure range from 0.75 to 5 kPa, the pressure/temperature sensor sustains excellent linearity (the R^2 coefficient is 0.98). The gauge factor of pressure sensing is 0.67 kPa^{-1} in the pressure range of 0.75–5 kPa (Fig. 3(a)). The wide pressure operating range and high sensitivity of the sensors benefit from the special surface structure of the electrodes and the sandwich structure of the sensors. The surface Gaussian distribution microstructure of the electrodes can effectively extend the linear range of pressure sensing. According to the working

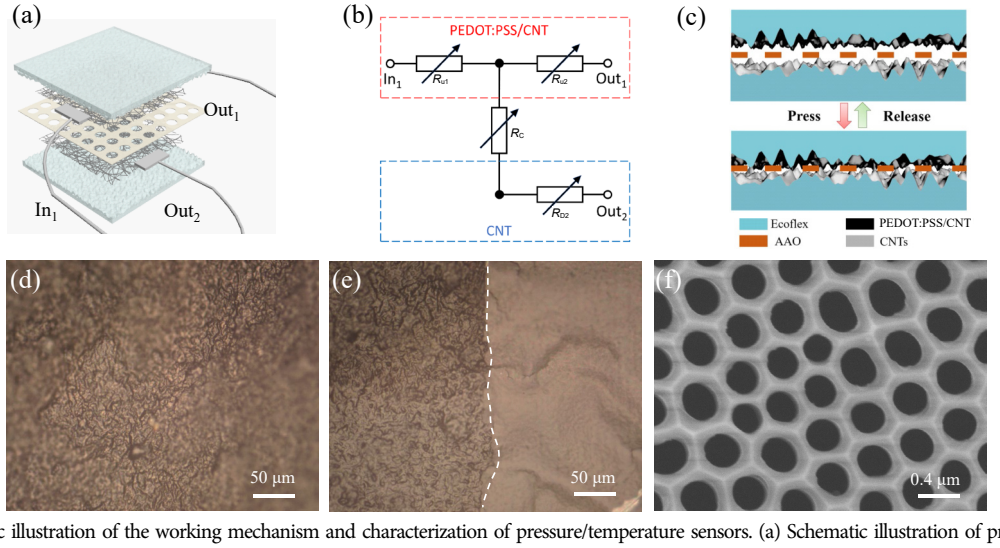

Figure 2 Schematic illustration of the working mechanism and characterization of pressure/temperature sensors. (a) Schematic illustration of pressure/temperature sensor structure. (b) Equivalent circuit of the sensor. (c) Schematic illustration of the working mechanism of pressure sensing. (d) Optical image of CNT film on Ecoflex substrate with surface microstructure. (e) Optical image of CNT film on Ecoflex substrate partially covered with AAO (right half). (f) SEM image of AAO membrane.

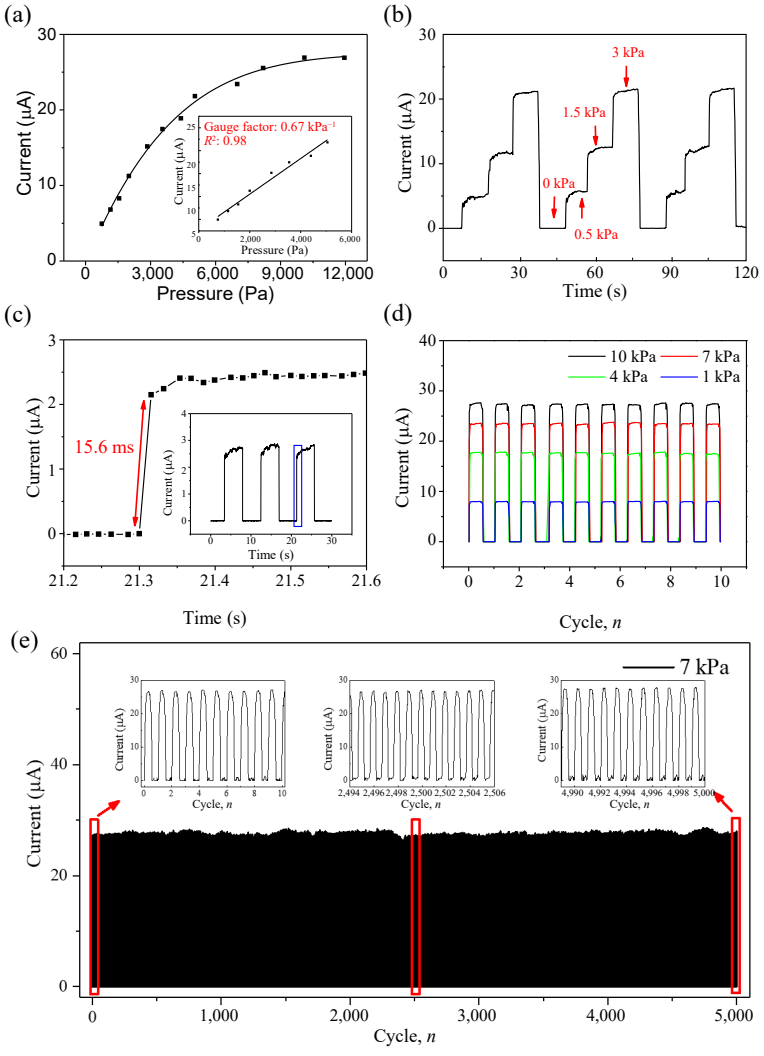

Figure 3 Characterization of the pressure sensing properties of the pressure/temperature sensor. (a) The current response of the sensor verse applied pressure. (b) The current response verse step increased pressure from 0 to 3 kPa. (c) Current–pressure response time of the sensor in pressure sensing. (d) Dynamic current responses under different pressures from 1 to 10 kPa. (e) Response stability under 7 kPa pressure in 5,000 cycles.

mechanism of the pressure sensors, we believe that its linear working range can be further improved by using an AAO membrane with no-uniform pores. For the sensor, the insulated AAO blocking layer can avoid conduction between the top and bottom electrodes in the "off" state of the pressure sensor, which could enhance the operating sensitivity. Furthermore, the sensor can measure small changes of applied pressure precisely. As shown in Fig. 3(b), the current response of the sensor can reflect the step change of applied pressure, which possesses great stability in three cycles. The response current of the sensor in Fig. 3(b) is slightly higher than that of Fig. 3(a) at the same pressure. This may be due to the samples prepared in different batches, resulting in some differences in performance. Besides, the sensor can measure the dynamic pressure signal, and the response time of the sensor is about 15.6 ms (Fig. 3(c)), which is comparable to the pressure sensor based on gold nanowires (17 ms) [45]. The current responses of the sensors under pressure ranging from 1 to 10 kPa under different pressures are easy to be distinguished and the current response of repeated cycles under the same pressure is consistent, as shown in Fig. 3(d). This sensor has good stability under both the low (750 Pa) and high (12 kPa) pressure ranges (Fig. S3 in the ESM). To further examine the long-term stability of the sensor in pressure sensing, the sensor has been run a 5,000 loading and unloading cycle test under the maximum applied pressure of 7 kPa. The current response of 5,000 cycles shows nearly no damping, as shown in Fig. 3(e).

Apart from pressure sensing, the temperature sensing characteristic of the pressure/temperature sensor is showed in Fig. 4(a). By using PEDOT:PSS/CNT composite as the sensitive layer, the sensor can measure a temperature ranging from −50 to 150 °C. In temperatures ranging from −30 to 30 °C, the relative resistance is nearly linear to temperature. The temperature sensitivity and linearity in this temperature range are 1.41%/°C and 0.99, respectively (inset of Fig. 4(a)). The temperature sensitivity of the sensors was calculated by the following equation: $S = \delta(\Delta R/R_0)/\delta T$, where ΔR is the resistance change from Out_1 of the sensor under temperature; R_0 is the resistance of the sensor at room temperature (20 °C), and T is the test temperature. The temperature sensitivity of the sensor at a temperature ranging from −50 to 150 °C is demonstrated in Fig. S4 in the ESM. These results show that the PEDOT:PSS/CNT composite has a negative temperature coefficient (NTC), which was also reported in several other papers [31, 32, 46]. For comparison, we have fabricated some temperature sensors by using CNT, PEDOT:PSS, and PEDOT:PSS/CNT as electrodes, respectively. The temperature sensitivities of CNT, PEDOT:PSS, and PEDOT:PSS/CNT are 0.04%/°C, 0.24%/°C, and 0.50%/°C, respectively (Fig. 4(b)). It shows that CNT and PEDOT:PSS are both negative temperature coefficient materials. After compounding, PEDOT:PSS/CNT composite has a larger temperature coefficient than both CNT and PEDOT:PSS, which is likely because of the potential electron hopping at the PEDOT:PSS/CNT interface [47].

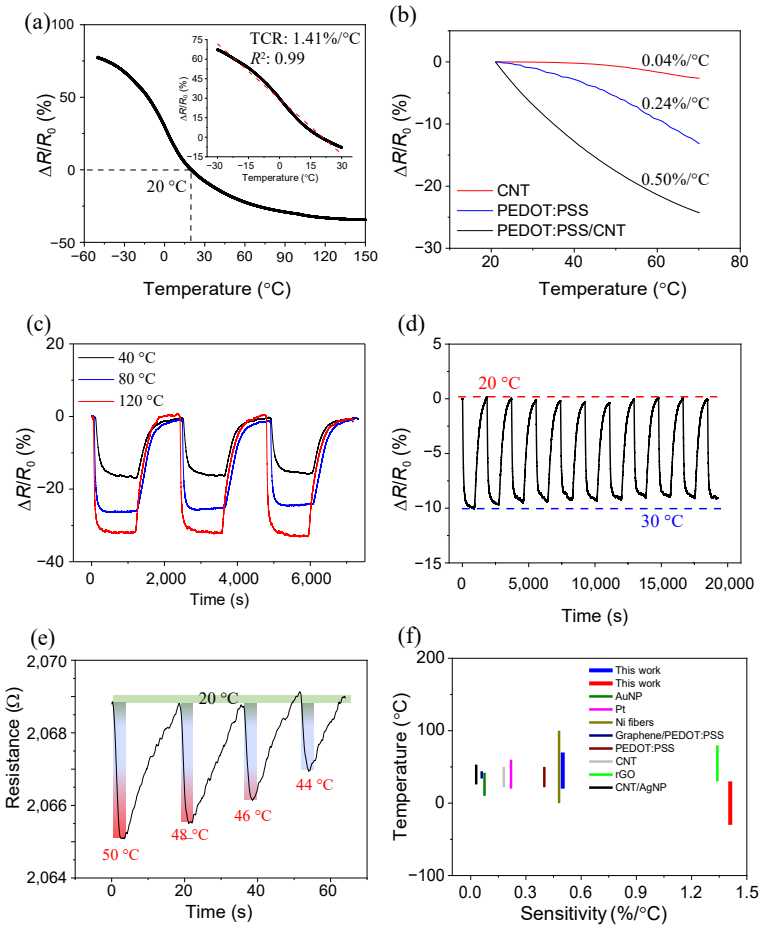

Figure 4 Characterization of temperature sensing properties of the sensor. (a) Relative resistance response of pressure/temperature sensor verse temperature. (b) The relative resistance change of the sensor with CNT, PEDOT:PSS, and PEDOT:PSS/CNT electrodes, respectively. (c) Relative resistance response of pressure/temperature sensor in 3 cycles from 20 to 40, 80, and 120 °C. (d) Relative resistance response in 10 heating and cooling cycles. (e) The relative resistance change of pressure/temperature sensor during a brief contact (2 s) with a glass of hot water. (f) Comparison of temperature sensitivity and working range between our pressure/temperature sensor and the recently reported temperature sensors.

The results of the cycle test of the sensors under the temperature varying from 20 to 40 °C, 20 to 80 °C, and 20 to 120 °C indicate that the sensors also have high stability for temperature sensing (Fig. 4(c)). The *I*/*V* curves of the pressure/temperature sensor are linear at 20, 40, 80, and 120 °C (Fig. S5 in the ESM). The most common temperature of electronic skin application is about 20–30 °C, which makes it important to improve the sensitivity and linearity of temperature sensors in this range. The relative resistance response of the sensor in temperature ranging from 20 to 30 °C is shown in Fig. 4(d). The temperature sensitivity in this temperature range is about 0.8 %/°C, which is high enough for practical application. It further shows that the sensor has high stability for temperature sensing. We can measure the temperature of any object in the detection range by using this sensor. Figure 4(e) shows the resistance change of the sensor during a short contact (2 s) with different temperatures of hot water. The resistance changing rate depends on the temperature. As shown in Fig. 4(e), when contacting with 50 °C hot water, the resistance decreases 2 Ω/s. When contacting with 44 °C hot water, the resistance decreased by 1.2 Ω/s. These indicate that the sensors have a fast response to temperature changes. The temperature sensitivity of our sensor is compared with other temperature sensors, as illustrated in Fig. 4(f). It shows that our sensor possesses high sensitivity compared with temperature sensors based on other materials such as Au nanoparticle (AuNP) [48], Pt [49], Ni fibers [50], graphene/PEDOT:PSS [46], PEDOT:PSS [31], CNT [31], reduced graphene oxide (rGO) [25], and CNT/Ag nanoparticle (AgNP) [32].

The high sensitivity pressure/temperature sensors can be used in flexible electronics and human-machine interaction for pressure and temperature monitoring. For example, a hand holds a beaker with hot water, and four pressure/temperature sensors have been mounted on different fingertips (Fig. 5(a)). These sensors can sense the pressure stimuli and temperature stimuli simultaneously. The performance of these sensors under different pressures and temperatures is shown in Fig. 5(b). It indicates that the response current increases with increasing temperature and pressure. At the same temperature (40 °C), the current at a pressure of 8 kPa is eight times that at a pressure of 2 kPa. At the same pressure (2 kPa), the current is 49.9 μA at 80 °C, but the current is only 6.2 μA at 40 °C. These further indicate that the sensor has a high resolution for pressure and temperature stimuli. Theoretically, we can decouple the temperature and pressure stimuli through only one output response current signal by calibrating the current value as well as the change rate of current with pressure. As shown in Fig. 5(c), the pressure/temperature sensor can detect a tiny pressure such as the gravity of a soybean. Besides, the current response is different if the temperature changes from 20 to 40 °C. Since the sensor has a fast response speed, it can distinguish the double click of the mouse (Fig. 5(d)). The time interval between two times of mouse clicks in this test is about 160 ms, which has reached the limit of finger movement. Furthermore, by this direct stamping method, we can use a copper mask to fabricate PEDOT:PSS/CNT strips for the sensor matrix. We have constructed a pressure sensing array that can measure the pressure distribution in high resolution (2.5 mm^2) (Fig. 5(e)). It can also detect both the magnitude and the position of applied pressure, which is useful in the touch panel (Fig. 5(f)).

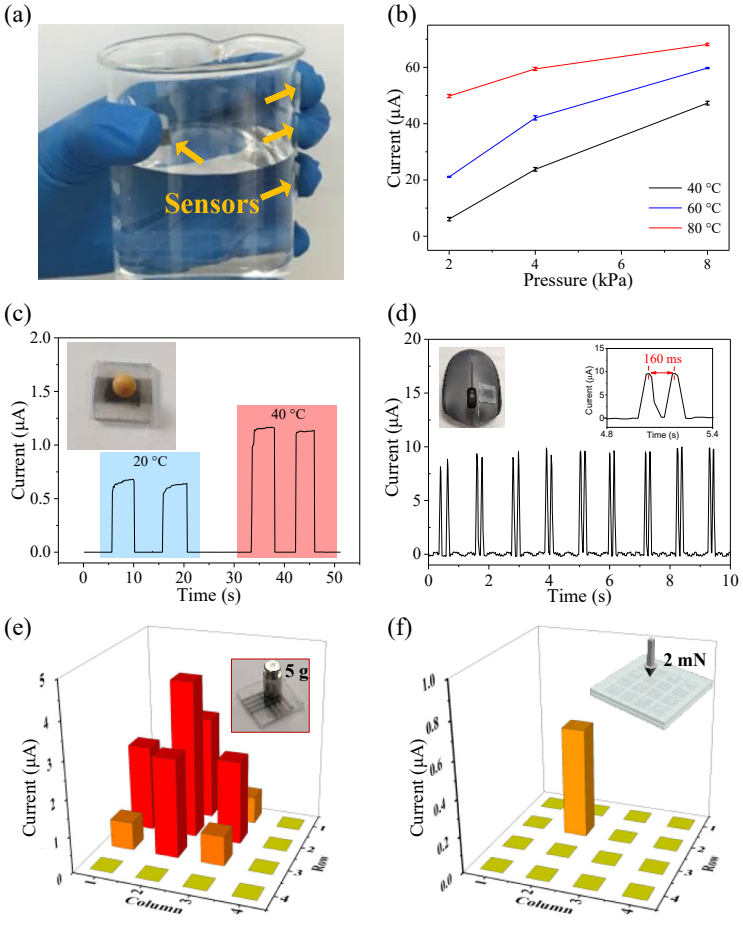

Figure 5 Several applications of the pressure/temperature sensor. (a) Photograph of the pressure/temperature sensors. (b) The current responses of the pressure/temperature sensor under different pressures and temperatures. (c) The current responses to soya bean under different temperatures. (d) The current response to rapid mechanical stimulation signal (mouse clicks). (e) The current response of the sensor array corresponding to the pressure distribution. (f) The current response of sensor array under single-point applied pressure of 2 mN.

4 Conclusions

In summary, by direct stamping method, we have fabricated a multifunctional sensor, which can measure pressure and temperature simultaneously. This sensor possesses high sensitivity in both pressure sensing (0.67 kPa^{-1}) and temperature sensing (1.41%/°C). Besides, the stability of our pressure/temperature sensor in 5,000 cycles is excellent. This pressure/temperature sensor can detect and measure tiny pressure stimuli and temperature variations. It suggests that our sensor will have great potential applications in flexible electronic devices.

Acknowledgments

This work was financially supported by the National Natural Science Foundation of China (No. 52072415), Guangdong Basic and Applied Basic Research Foundation (No. 2021A1515012387), and the Science and Technology Program of Guangzhou (No. 201904010450).

Electronic Supplementary Material: Supplementary material (electrical and electromechanical properties of the transferred CNT film fabricated by different processes) is available in the online version of this article at https://doi.org/10.1007/s12274-021-3906-x.

References

[1] Chen, Z. F.; Wang, Z.; Li, X. M.; Lin, Y. X.; Luo, N. Q.; Long, M. Z.; Zhao, N.; Xu, J. B. Flexible piezoelectric-induced pressure sensors for static measurements based on nanowires/graphene heterostructures. *ACS Nano* **2017**, *11*, 4507–4513.

[2] Shi, J. D.; Wang, L.; Dai, Z. H.; Zhao, L. Y.; Du, M. D.; Li, H. B.; Fang, Y. Multiscale hierarchical design of a flexible piezoresistive pressure sensor with high sensitivity and wide linearity range. *Small* **2018**, *14*, 1800819.

[3] Wan, C. J.; Chen, G.; Fu, Y. M.; Wang, M.; Matsuhisa, N.; Pan, S. W.; Pan, L.; Yang, H.; Wan, Q.; Zhu, L. Q. et al. An artificial sensory neuron with tactile perceptual learning. *Adv. Mater.* **2018**, *30*, 1801291.

[4] Boutry, C. M.; Kaizawa, Y.; Schroeder, B. C.; Chortos, A.; Legrand, A.; Wang, Z.; Chang, J.; Fox, P.; Bao, Z. A. A stretchable and biodegradable strain and pressure sensor for orthopaedic application. *Nat. Electron.* **2018**, *1*, 314–321.

[5] Dong, K.; Wu, Z. Y.; Deng, J. N.; Wang, A. C.; Zou, H. Y.; Chen, C. Y.; Hu, D. M.; Gu, B. H.; Sun, B. Z.; Wang, Z. L. A Stretchable yarn embedded triboelectric nanogenerator as electronic skin for biomechanical energy harvesting and multifunctional pressure sensing. *Adv. Mater.* **2018**, *30*, 1804944.

[6] Chen, S.; Jiang, K.; Lou, Z.; Chen, D.; Shen, G. Z. Recent developments in graphene-based tactile sensors and E-skins. *Adv. Mater. Technol.* **2018**, *3*, 1700248.

[7] Yin, B.; Liu, X. M.; Gao, H. Y.; Fu, T. D.; Yao, J. Bioinspired and bristled microparticles for ultrasensitive pressure and strain sensors. *Nat. Commun.* **2018**, *9*, 5161.

[8] Chou, H. H.; Nguyen, A.; Chortos, A.; To, J. W. F.; Lu, C. E.; Mei, J. G.; Kurosawa, T.; Bae, W. G.; Tok, J. B.; Bao, Z. A. A chameleon-inspired stretchable electronic skin with interactive colour changing controlled by tactile sensing. *Nat. Commun.* **2015**, *6*, 8011.

[9] Park, J.; Lee, Y.; Hong, J.; Ha, M.; Jung, Y. D.; Lim, H.; Kim, S. Y.; Ko, H. Giant tunneling piezoresistance of composite elastomers with interlocked microdome arrays for ultrasensitive and multimodal electronic skins. *ACS Nano* **2014**, *8*, 4689–4697.

[10] Tian, H.; Shu, Y.; Wang, X. F.; Mohammad, M. A.; Bie, Z.; Xie, Q. Y.; Li, C.; Mi, W. T.; Yang, Y.; Ren, T. L. A graphene-based resistive pressure sensor with record-high sensitivity in a wide

pressure range. *Sci. Rep.* **2015**, *5*, 8603.
[11] Chun, S.; Kim, Y.; Oh, H. S.; Bae, G.; Park, W. A highly sensitive pressure sensor using a double-layered graphene structure for tactile sensing. *Nanoscale* **2015**, *7*, 11652–11659.
[12] Jian, M. Q.; Xia, K. L.; Wang, Q.; Yin, Z.; Wang, H. M.; Wang, C. Y.; Xie, H. H.; Zhang, M. C.; Zhang, Y. Y. Flexible and highly sensitive pressure sensors based on bionic hierarchical structures. *Adv. Funct. Mater.* **2017**, *27*, 1606066.
[13] You, I.; Mackanic, D. G.; Matsuhisa, N.; Kang, J.; Kwon, J.; Beker, L.; Mun, J.; Suh, W.; Kim, T. Y.; Tok, J. B. H. et al. Artificial multimodal receptors based on ion relaxation dynamics. *Science* **2020**, *370*, 961–965.
[14] Wang, Y.; Wu, H. T.; Xu, L.; Zhang, H. N.; Yang, Y.; Wang, Z. L. Hierarchically patterned self-powered sensors for multifunctional tactile sensing. *Sci. Adv.* **2020**, *6*, eabb9083.
[15] Tao, X. L.; Liao, S. L.; Wang, Y. P. Polymer-assisted fully recyclable flexible sensors. *EcoMat* **2021**, *3*, e12083.
[16] Lu, Y.; Biswas, M. C.; Guo, Z. H.; Jeon, J. W.; Wujcik, E. K. Recent developments in bio-monitoring via advanced polymer nanocomposite-based wearable strain sensors. *Biosens. Bioelectron.* **2019**, *123*, 167–177.
[17] Amjadi, M.; Kyung, K. U.; Park, I.; Sitti, M. Stretchable, skin-mountable, and wearable strain sensors and their potential applications: A review. *Adv. Funct. Mater.* **2016**, *26*, 1678–1698.
[18] Kong, J. H.; Jang, N. S.; Kim, S. H.; Kim, J. M. Simple and rapid micropatterning of conductive carbon composites and its application to elastic strain sensors. *Carbon* **2014**, *77*, 199–207.
[19] Lu, N. S.; Lu, C.; Yang, S. X.; Rogers, J. Highly sensitive skin-mountable strain gauges based entirely on elastomers. *Adv. Funct. Mater.* **2012**, *22*, 4044–4050.
[20] Oh, J.; Yang, J. C.; Kim, J. O.; Park, H.; Kwon, S. Y.; Lee, S.; Sim, J. Y.; Oh, H. W.; Kim, J.; Park, S. Pressure insensitive strain sensor with facile solution-based process for tactile sensing applications. *ACS Nano* **2018**, *12*, 7546–7553.
[21] Li, Q.; Zhang, L. N.; Tao, X. M.; Ding, X. Review of flexible temperature sensing networks for wearable physiological monitoring. *Adv. Healthc. Mater.* **2017**, *6*, 1601371.
[22] Ismail, A. S.; Mamat, M. H.; Rusop, M. Humidity Sensor—A review of nanostructured zinc oxide (ZnO)-based humidity sensor. *Appl. Mech. Mater.* **2015**, *773–774*, 706–710.
[23] Wang, C. Y.; Xia, K. L.; Zhang, M. C.; Jian, M. Q.; Zhang, Y. Y. An All-silk-derived dual-mode E-skin for simultaneous temperature-pressure detection. *ACS Appl. Mater. Interfaces* **2017**, *9*, 39484–39492.
[24] Zhang, L. C.; Jiang, Y.; Gao, H. C.; Jia, J. S.; Cui, Y.; Wang, S. M.; Hu, J. Simultaneous measurements of temperature and pressure with a dual-cavity Fabry-Perot sensor. *IEEE Photonics Technol. Lett.* **2019**, *31*, 106–109.
[25] Trung, T. Q.; Ramasundaram, S.; Hwang, B. U.; Lee, N. E. An all-elastomeric transparent and stretchable temperature sensor for body-attachable wearable electronics. *Adv. Mater.* **2016**, *28*, 502–509.
[26] Kickhofel, J.; Yang, J. M.; Prasser, H. M. Designing a high temperature high pressure mesh sensor. *Nucl. Eng. Des.* **2018**, *336*, 122–128.
[27] Graz, I.; Krause, M.; Bauer-Gogonea, S.; Bauer, S.; Lacour, S. P.; Ploss, B.; Zirkl, M.; Stadlober, B.; Wagner, S. Flexible active-matrix cells with selectively poled bifunctional polymer-ceramic nanocomposite for pressure and temperature sensing skin. *J. Appl. Phys.* **2009**, *106*, 034503.
[28] Yang, Y. J.; Cheng, M. Y.; Chang, W. Y.; Tsao, L. C.; Yang, S. A.; Shih, W. P.; Chang, F. Y.; Chang, S. H.; Fan, K. C. An integrated flexible temperature and tactile sensing array using PI-copper films. *Sensor. Actuat. A:Phys.* **2008**, *143*, 143–153.
[29] Someya, T.; Kato, Y.; Sekitani, T.; Iba, S.; Noguchi, Y.; Murase, Y.; Kawaguchi, H.; Sakurai, T. Conformable, flexible, large-area networks of pressure and thermal sensors with organic transistor active matrixes. *Proc. Natl. Acad. Sci. USA* **2005**, *102*, 12321–12325.
[30] Zhao, X. H.; Ma, S. N.; Long, H.; Yuan, H. Y.; Tang, C. Y.; Cheng, P. K.; Tsang, Y. H. Multifunctional sensor based on porous carbon derived from metal-organic frameworks for real time health monitoring. *ACS Appl. Mater. Interfaces* **2018**, *10*, 3986–3993.
[31] Honda, W.; Harada, S.; Arie, T.; Akita, S.; Takei, K. Wearable, human-interactive, health-monitoring, wireless devices fabricated by macroscale printing techniques. *Adv. Funct. Mater.* **2014**, *24*, 3299–3304.
[32] Harada, S.; Honda, W.; Arie, T.; Akita, S.; Takei, K. Fully printed, highly sensitive multifunctional artificial electronic whisker arrays integrated with strain and temperature sensors. *ACS Nano* **2014**, *8*, 3921–3927.
[33] Cheng, Y.; Wang, R. R.; Sun, J.; Gao, L. A stretchable and highly sensitive graphene-based fiber for sensing tensile strain, bending, and torsion. *Adv. Mater.* **2015**, *27*, 7365–7371.
[34] Ge, J.; Yao, H. B.; Wang, X.; Ye, Y. D.; Wang, J. L.; Wu, Z. Y.; Liu, J. W.; Fan, F. J.; Gao, H. L.; Zhang, C. L. et al. Stretchable conductors based on silver nanowires: improved performance through a binary network design. *Angew. Chem.* **2013**, *125*, 1698–1703.
[35] Lu, L. J.; Wei, X. D.; Zhang, Y.; Zheng, G. Q.; Dai, K.; Liu, C. T.; Shen, C. Y. A flexible and self-formed sandwich structure strain sensor based on AgNW decorated electrospun fibrous mats with excellent sensing capability and good oxidation inhibition properties. *J. Mater. Chem. C.* **2017**, *5*, 7035–7042.
[36] Lee, J.; Kim, S.; Lee, J.; Yang, D.; Park, B. C.; Ryu, S.; Park, I. A stretchable strain sensor based on a metal nanoparticle thin film for human motion detection. *Nanoscale* **2014**, *6*, 11932–11939.
[37] Lipomi, D. J.; Vosgueritchian, M.; Tee, B. C. K.; Hellstrom, S. L.; Lee, J. A.; Fox, C. H.; Bao, Z. A. Skin-like pressure and strain sensors based on transparent elastic films of carbon nanotubes. *Nat. Nanotechnol.* **2011**, *6*, 788–792.
[38] Muth, J. T.; Vogt, D. M.; Truby, R. L.; Mengüç, Y.; Kolesky, D. B.; Wood, R. J.; Lewis, J. A. Embedded 3D printing of strain sensors within highly stretchable elastomers. *Adv. Mater.* **2014**, *26*, 6307–6312.
[39] Michelis, F.; Bodelot, L.; Bonnassieux, Y.; Lebental, B. Highly reproducible, hysteresis-free, flexible strain sensors by inkjet printing of carbon nanotubes. *Carbon* **2015**, *95*, 1020–1026.
[40] Zeng, S. S.; Zhang, D. Y.; Huang, W. H.; Wang, Z. F.; Freire, S. G.; Yu, X. Y.; Smith, A. T.; Huang, E. Y.; Nguon, H.; Sun, L. Y. Bio-inspired sensitive and reversible mechanochromisms via strain-dependent cracks and folds. *Nat. Commun.* **2016**, *7*, 11802.
[41] Wang, M.; Wang, W.; Leow, W. R.; Wan, C. J.; Chen, G.; Zeng, Y.; Yu, J. C.; Liu, Y. Q.; Cai, P. Q.; Wang, H. et al. Enhancing the matrix addressing of flexible sensory arrays by a highly nonlinear threshold switch. *Adv. Mater.* **2018**, *30*, 1802516.
[42] Gui, X. C.; Wei, J. Q.; Wang, K. L.; Cao, A. Y.; Zhu, H. W.; Jia, Y.; Shu, Q. K.; Wu, D. H. Carbon nanotube sponges. *Adv. Mater.* **2010**, *22*, 617–621.
[43] Liang, B. H.; Zhang, Z. A.; Chen, W. J.; Liu, D. W.; Yang, L. L.; Yang, R. L.; Zhu, H.; Tang, Z. K.; Gui, X. C. Direct patterning of carbon nanotube via stamp contact printing process for stretchable and sensitive sensing devices. *Nano-Micro Lett.* **2019**, *11*, 92.
[44] Chen, Y.; Gong, X. L.; Gai, J. G. Progress and challenges in transfer of large-area graphene films. *Adv. Sci.* **2016**, *3*, 1500343.
[45] Gong, S.; Schwalb, W.; Wang, Y. W.; Chen, Y.; Tang, Y.; Si, J.; Shirinzadeh, B.; Cheng, W. L. A wearable and highly sensitive pressure sensor with ultrathin gold nanowires. *Nat. Commun.* **2014**, *5*, 3132.
[46] Vuorinen, T.; Niittynen, J.; Kankkunen, T.; Kraft, T. M.; Mäntysalo, M. Inkjet-printed graphene/PEDOT:PSS temperature sensors on a skin-conformable polyurethane substrate. *Sci. Rep.* **2016**, *6*, 35289.
[47] Takei, K.; Honda, W.; Harada, S.; Arie, T.; Akita, S. Toward flexible and wearable human-interactive health-monitoring devices. *Adv. Healthc. Mater.* **2015**, *4*, 487–500.
[48] Huynh, T. P.; Haick, H. Self-healing, fully functional, and multiparametric flexible sensing platform. *Adv. Mater.* **2016**, *28*, 138–143.
[49] Dankoco, M. D.; Tesfay, G. Y.; Benevent, E.; Bendahan, M. Temperature sensor realized by inkjet printing process on flexible substrate. *Mater. Sci. Eng. :B* **2016**, *205*, 1–5.
[50] Husain, M. D.; Kennon, R. Preliminary investigations into the development of textile based temperature sensor for healthcare applications. *Fibers* **2013**, *1*, 2–10.